Energy transfer and constrained simulations in isotropic turbulence

By J. Jiménez[1]

1. Motivation

The defining characteristic of turbulent flows is their ability to dissipate energy, even in the limit of zero viscosity. The Euler equations, if constrained in such a way that the velocity derivatives remain bounded, conserve energy. But when they arise as the limit of the Navier-Stokes (NS) equations, when the Reynolds number goes to infinity, there is persuasive empirical evidence that the gradients become singular as just the right function of Re for the dissipation to remain non-zero and to approach a well defined limit (Sreenivasan 1984). It is generally believed that this limiting value of the dissipation is a property of the Euler equations themselves, independent of the particular dissipative mechanism involved, and that it can be normalized with the large scale properties of the turbulent flow (e.g. the kinetic energy per unit volume $u'^2/2$, and the integral scale L) without reference to the Reynolds number or to other dissipative quantities (Batchelor 1953, §6). This is usually taken to imply that the low wave number end of the energy spectrum, far from the dissipative range, is also independent of the particular mechanism chosen to dispose of the energy transfer.

While these considerations have proved adequate in analyzing the solutions of the NS equations at different Reynolds numbers, they are recently being used in a more general context to predict the effect of different subgrid models in Large Eddy Simulations (LES) of turbulent flows. The LES equations are neither the Euler nor the NS equations. Because of the intrinsically finite capacity of computers, the Euler equations are first truncated to a relatively low number of degrees of freedom, generally much lower than that needed to represent the dissipative scales, and the missing dissipation is provided by the addition of a "subgrid" model whose goal is to mimic the effect on the large scales of the degrees of freedom that have been filtered in the original truncation. In most cases, the resulting model is very different from the quadratic viscosity characteristic of the NS equations, and the hope that it will approximate the behavior of the original high Reynolds number flow hinges on the belief that the dissipation independence observed empirically for the energy transfer mechanism of the NS equations will persist in the new systems.

This is, therefore, a good time to re-evaluate the original assumptions and the limits of their applicability. This will also give us a new tool to investigate the mechanism of the energy cascade itself and its relation to normal viscosity. It has always been an open question how much of NS turbulence is unique to the solutions

1 Also with the School of Aeronautics, Madrid.

of the NS equations, and what parts of it would be shared by other nonlinear systems of partial differential equations. The arguments outlined above suggest that the quadratic nonlinearity might be essential but that the dissipative model is not. While physical experiments with non-Newtonian fluids are difficult and relatively rare, numerical experiment with different viscosity models are commonplace and have been used for a long time to achieve higher Reynolds numbers that those obtainable with Direct Numerical Simulation, especially in two dimensional flows. As argued above, most LES computations also fall into this category. Although many of these simulations have been quite successful in approximating the results of experiments, relatively few detailed comparisons are available, and the presence in most cases of adjustable parameters makes the agreement less compelling.

Moreover, there is some experimental evidence that this dissipation independence is not complete in all cases. The addition of small concentrations of polymers in wall bounded flows is known to produce a dramatic decrease of skin friction (Berman 1978). Since skin friction for a given flow rate is directly proportional to energy dissipation, and since polymers are thought to act only on the small structures, that evidence is troubling. The same is true of riblets (Walsh 1990), which also modify friction even if they are small scale features. Finally, the friction coefficient of smooth-walled channels does not asymptote to a fixed value, even at the highest Reynolds numbers observed (Dean 1978). While wall bounded flows may be different from isotropic or free shear flows, most conspicuously because in the wall region the "local" Reynolds number can always be argued to be low, these observations should be taken into account when extending the results of the latter into the behavior of the former. In this work, we will only concern ourselves with the behavior of isotropic periodic numerical simulations of the Euler or LES equations and with their relation to NS turbulence.

Even in this case, we have to qualify our support for the hypothesis of complete independence of the large scale motions from the details of the small scales. It is well known that a consequence of an inviscid energy cascade is the famous Kolmogorov (1941) $E(k) \sim k^{-5/3}$ spectral law. Since this result is independent of viscosity, the arguments above would make it a property of the Euler equations. But it has been known for a long time that those equations have at least another power law equilibrium spectrum $E(k) \sim k^2$, corresponding to energy equipartition among the spectral modes (Lee 1952). In physical systems, flow fields with such a spectrum are highly singular and are not expected to be observable since any residual viscosity, however small, would damp the high wave numbers and force a decreasing spectral tail. These solutions are, however, consistent with the inviscid equations, and they reappear as soon as the possibility of a singularity is removed. In fact, as soon as the Euler equations are truncated to a finite number of degrees of freedom, they tend spontaneously to the equipartition solution (Fig. 1). This is relevant to our discussion because it shows that the effect of dissipation in the NS equations is not only to fix the length scale of the viscous limit (the Kolmogorov scale η), but to select the "desired" $k^{-5/3}$ spectrum away from the "contamination" of the equipartition component k^2. It is not immediately clear whether other dissipation mechanisms
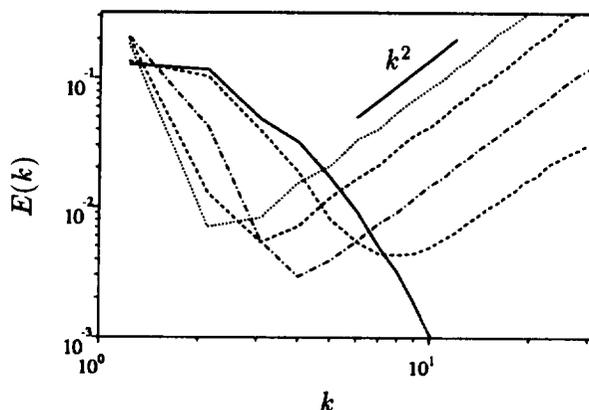
FIGURE 1.   Evolution of the three-dimensional energy spectrum of the Euler equations in a 64^3 numerical box. Time increases with energy at high wave numbers. The initial flow field is fully developed turbulence from a NS simulation (solid line).

are able to do the same.

In the following sections, we present some numerical experiments on the effect of substituting different dissipation models into the truncated Euler equations. We will see that the effect is mainly felt in the "near dissipation" range of the energy spectrum, but that this range can be quite wide in some cases, contaminating a substantial range of wave numbers. In the process, we will develop a "practical" approximation to the subgrid energy transfer in isotropic turbulence, and we will gain insight into the structure of the nonlinear interactions among turbulent scales of comparable size, and into the nature of energy backscatter. Some considerations on future research directions are offered at the end.

2. Inertial simulations

2.1 The truncated Euler equations

This section of the paper will deal with attempts to model the inertial spectral range of isotropic turbulence at infinite Reynolds number.

Our first numerical experiment simulates spatially periodic turbulence with no viscosity. The numerical method is fully spectral, using primitive variables u, p, with dealiasing achieved by spherical masking in Fourier space and phase shifting (Rogallo, 1981, see description in Canuto *et al.*, 1987). The resolutions quoted for the different simulations reflect the number of real Fourier modes in each direction before dealiasing; the number of actual useful modes in the power spectra, k_{max}, is slightly less than half that number. The Fourier expansion functions are $\exp(ik_j x_j)$, $|k_j| = 0, 1, \ldots, N/2$, so that the length of the box side is always 2π. The time stepping procedure is second-order Runge-Kutta for the nonlinear terms and an analytic integrating factor for the viscous ones, when present. The time step is automatically controlled to satisfy the numerical stability condition. Unless stated otherwise, all experiments are forced to achieve a statistically stationary flow, and

the results presented are long term averages, usually taken over periods of the order of one or two large scale turnover times after stationarity is achieved. Forcing is achieved by multiplying all the modes in a spherical spectral shell by an appropriate real factor at every time step until the total kinetic energy contained in the shell matches a predetermined value. The energy dissipation is measured by monitoring the multiplying factor.

The first inviscid simulation was carried out at 64^3 resolution, and forcing was used to fix the energy in the low wavenumber shell $k = |\mathbf{k}| \leq 2.5$. The simulation was initiated from a fully resolved NS forced field at the same resolution and with $k_{max}\eta \approx 2$, where η is the Kolmogorov scale, with a microscale Reynolds number $Re_\lambda \approx 36$ (Jiménez *et al.* 1993). It was not carried to a stationary state due to time limitations. As expected, energy accumulated immediately at the high wavenumber end of the spectrum, which took a characteristic k^2 shape. Several stages of its evolution are shown in Fig. 1. The absence of an appreciable numerical viscosity was checked by monitoring the skewness of the velocity derivatives, which rose from an initial value of approximately -0.5, characteristic of NS turbulence, to a final one of $\pm 10^{-3}$.

The inability to obtain a dissipative spectrum from the truncated Euler equations themselves shows that an extra condition is needed in the simulation. Since *two* possible similarity solutions exist, *two* conditions have to be used to decide the proportion in which they enter in the final solution. A useful model in which to explore what practical conditions might be most appropriate is the "diffusion" approximation to turbulent energy transfer proposed by Leith (1967). He obtains a differential equation for $E(k)$ as a function of time and wave number

$$\partial E/\partial t + \partial \epsilon/\partial k = -2\nu k^2 E. \tag{1a}$$

where the dissipation ϵ appears as an energy flux in spectral space, and is given by

$$\epsilon = -k^{13/2}\frac{\partial}{\partial k}k^{-3}E^{3/2}. \tag{1b}$$

Equation (1b) was constructed to have the solutions k^2 and $k^{-5/3}$ in the inviscid steady state limit and can be derived from an energy shell model with both forward and backward scatter, in the limit of infinitely thin spectral shells (Bell and Nelkin, 1978). The two similarity solutions are

$$\epsilon = \text{const.}, \qquad E = (2\epsilon/13)^{2/3}k^{-5/3}, \tag{2}$$

and

$$\epsilon = 0, \qquad E \sim k^2. \tag{3}$$

Since eq. (1) is nonlinear, the final stationary inviscid spectrum is not simply a linear combination of both solutions, but

$$E = (2\epsilon/13)^{2/3}\left(k^{-5/2} + ak^3\right)^{2/3}. \tag{4}$$
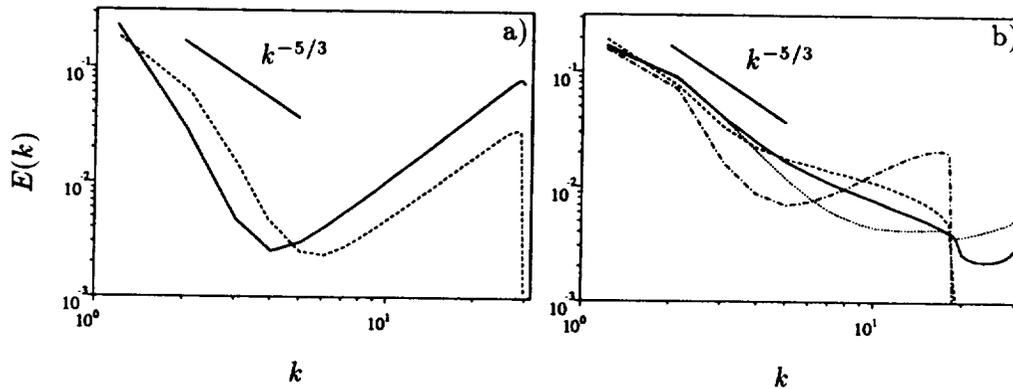
FIGURE 2. Three dimensional energy spectra for Euler simulations in which the total energy at high wavenumbers, $k > k_c$, is kept fixed, in addition to the forcing at low wave numbers. (a) $k_c = k_{max} - 1$. ———— : energy in damped shell, $E_c = 7.5 \times 10^{-2}$; ———— : 10^{-3}. (b) $k_c = 2k_{max}/3$. ········ line: $E_c = 0.05$; ———— : approx. 0.027, see text; ———— : 5×10^{-3}; —·—·— : 5×10^{-4}

This solution has the right Kolmogorov form up to an (arbitrary) constant but contains an extra term coming from the equipartition component. Two conditions are needed to adjust the dissipation, ϵ, and the constant a. Note that in the model as well as in the actual flow, the equipartition spectrum is conservative. Because the behaviors of the two spectra are very different, one of them increasing and the other decreasing with k, the two constants are determined almost independently by disjoint wave number ranges. Fixing the energy in a low wave number shell essentially fixes the dissipation because k^2 is small in that range, while fixing the energy in a high wave number shell does the same for the equipartition component. This is consistent with the common statement that the large scales of the flow fix the dissipation, but it is true only if the equipartition component, a, can be guaranteed to be $O(1)$. The previous inviscid example shows that this only happens if the energy at high wave numbers has been forced to be small. The role of viscosity, from the point of view of the large scales, can be seen as that of avoiding the accumulation of energy at high wavenumbers and thus of controlling the k^2 component of the spectrum. In general, spectra with an insufficient dissipation mechanism look "almost right" at low wave numbers but have a large "hook" at high wave numbers, where the k^2 component takes over. Small spectral hooks of this kind are common in the last few wave numbers of direct numerical simulations.

2.2 Constrained simulations

Figure 2a shows the results of two attempts at fixing the energy both in the high and in the low spectral shells for a direct Euler simulation. The numerical parameters and the forcing scheme in the low wave numbers are exactly the same as for Fig. 1, but the code also adjusts independently the last spectral shell (of width

$\Delta k = 1$) by multiplying all the modes in it by a new damping factor, computed every time step, that brings the total energy in the shell to the desired level. This proves to be effective only when the energy chosen is high enough but fails if it is too small, in which case the rest of the spectrum decouples from the damped shell. A little thought shows that too small an energy in the high wave numbers inhibits the energy transfer and that the next lower shell cannot dump energy into it fast enough. This is no more than saying that the Reynolds stresses, and the turbulent energy transfer, can only work if there are small scales to generate them, and that the dissipation of a laminar flow is much smaller. The result is an accumulation of energy similar to the one in the inviscid case. In fact, the limit in which the energy in the last shell is set exactly to zero is numerically equivalent to de-aliasing, and it would produce the same result as the unconstrained simulations in Fig. 1.

Controlling the energy over a thicker shell is more efficient since the lower modes have more spectral triads into which the energy can be transferred (or more active small scales). The result of fixing, in the same way as before, the total energy contained in all the modes with wave numbers $k > k_c = 2k_{max}/3$ is shown in Fig. 2b. It is now possible to control the energy of the high modes almost well enough to obtain a $k^{-5/3}$ extrapolation from the modes that are completely resolved by the simulation. The solid line in Fig. 2b is defined in that way; the energy above k_c is controlled at each step to coincide with the value it would have if its spectrum was a smooth inertial extrapolation of $E(k_c)$. That choice seems to be close to optimal from the point of view of obtaining a $k^{-5/3}$ over most of the inviscid scales. However, in this case also, an attempt to make the energy too small in the damped shell gross contamination of the spectrum with the equipartition component.

In all these simulations, the resolved scales are inviscid. In Fig. 1, all the spectral modes, except those in the lower forced shell, satisfy the Euler equations, and since there is no energy dissipation, the solution tends to equipartition. In the simulations in Fig. 2, only those modes with $k \leq k_c$ satisfy the inviscid equations. They receive energy from the lower forced shell and lose it to those modes above k_c, where it is removed every time step by the damping factor. This factor acts as an effective viscosity which is zero for all modes below k_c, but which is active above that threshold and which can be considered as an extreme case of wavenumber dependent hyperviscosity.

Fornberg (1977) used a similar simulation scheme to compute two dimensional turbulence. He let the enstrophy in a high shell grow for some time under the effect of the cascade and zeroed it periodically. The present scheme is probably a better representation of the true cascade dynamics in that it gives the flow a stationary energy reservoir with which to interact

In both schemes, the effect of the damped high-wavenumber shell is to provide a spectral bucket into which energy can be dumped naturally by the nonlinear interactions. It appears from the results of the simulations that a simple uniform damping factor, which adjusts the amplitudes of the small scale modes but does not modify their phase relationships, provides an approximation to the small scale flow that is good enough to produce a reasonably accurate level of energy transfer

into the damped shell. The key seems to be having the right amount of energy in that shell to produce the correct cascade rate. This suggests that an ideal transfer could be obtained if the energy spectrum in the damped shell was adjusted to follow exactly the $k^{-5/3}$ law.

A similar experiment was performed by (She & Jackson 1993, Zhou 1993). Both investigators constrained the entire spectrum to follow exactly the $k^{-5/3}$ law and studied different aspects of the energy transfer. In both cases, the correct scaling behaviors were observed and the Kolmogorov constant fell in the range of the experimental values. Shtilman and Chasnov (1992) also studied a constrained Euler system in which the spectrum was forced to remain exactly equal to that of a direct simulation of the same flow, run in parallel at higher resolution. Their goal was to determine whether the statistics of the constrained flow would be similar to those of the DNS field at the same time when filtered down to the same resolution. The correspondence was shown to be only approximate, especially for the higher statistical moments, but the low order statistics, those involved in the energy transfer mechanism, agreed well.

Our goal is different. We are not only trying to understand the degree to which the constrained system approximates locally the energy transfer, but also to determine whether an unconstrained system can be made to simulate the inviscid inertial spectrum by providing it with a downstream spectral "boundary condition" which absorbs energy in the right way. If this turns out to be possible, the unconstrained system might better approximate the statistics of the large scales, even though those of the small scales are only accurate to the extent of providing a correct energy sink. Such a scheme also offers a better chance of being adaptable to the study of inhomogeneous turbulent flows. We are therefore interested in constraining only a partial spectral shell at high wave numbers to a spectrum that is the $k^{-5/3}$ extrapolation of the energy in the last fully resolved shell k_c.

This was done for the dotted line in Fig. 3. The modes in $k > k_c = k_{max}/2$ were divided into sub-shells of thickness $\Delta k = 1$, and an independent damping factor was computed for each sub-shell at each time step to bring the spectrum to the form $E(k, t) = E(k_c, t)(k_c/k)^{5/3}$. As expected from the previous discussion, the behavior of the whole spectrum and not just that of the forced part was much closer to inertial than before. When the compensated spectrum is plotted in linear coordinates, however, it is seen that the result is still not perfect (Fig. 3b). A perfect inertial spectrum in this representation would be strictly equal to the Kolmogorov constant.

2.3 Turbulent viscosity

What are still missing are the nonlinear interactions involving scales smaller than those at the high end of the damped shell, which are not resolved in the simulation. Those interactions, linking the unconstrained modes with those in the sub-grid scales, act across a spectral gap imposed by the damped shell, and it is generally accepted (Kraichnan 1976, Yoshizawa 1982) that under those circumstances the effect of the small scales is equivalent to that of a constant eddy viscosity. The presence in filtered DNS fields of an eddy viscosity plateau at wave numbers one or
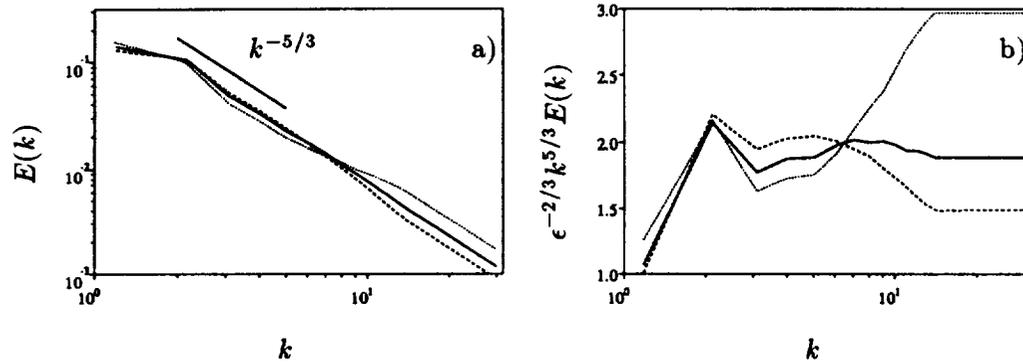
FIGURE 3.   Three dimensional energy spectra for Euler simulations in which the energy spectrum in the high wavenumber shell, $k > k_{max}/2$ is adjusted continuously to $k^{-5/3}$, in addition to a constant eddy viscosity and to the forcing at low wave numbers. (a) Uncompensated, (b) Normalized. $\cdots\cdots$: normalized eddy viscosity, $\alpha/\alpha_0 = 0$; ——— : 0.8; - - - - : 1.4.

more octaves lower than the filter width has been confirmed experimentally (Lesieur and Rogallo 1989). From dimensional considerations (Kraichnan 1976), the viscosity coefficient can be written as

$$\nu_e = \alpha \, [E(k_{max})/k_{max}]^{1/2}. \tag{5}$$

The normalized eddy viscosity α can be evaluated within the EDQNM approximation for infinite Reynolds number as $\alpha_0 \approx 0.267$ (Lesieur, 1990, pg. 324). This value assumes that the energy spectrum is strictly inertial beyond k_{max}, with a Kolmogorov constant of 1.4. The effect of adding this viscosity to the previous simulation is shown in Fig. 3. All modes are first marched according to the NS equations, with the viscosity given by rescaled to $k^{-5/3}$. Different values of α produce slightly different results, but the spectrum seems to fit best a single $k^{-5/3}$ law for a value slightly smaller than the EDQNM result, $\alpha \approx 0.214 = 0.8\alpha_0$. The corresponding Kolmogorov constant is in the range 1.8-1.9 (see Fig. 3b), in excellent agreement with that obtained in (She & Jackson 1993). This value is somewhat larger than the usually accepted one of 1.5, and the reason for the discrepancy is not clear. Zhou (1993) obtains a value of approximately 1.5 using a method which is conceptually similar to the one in (She & Jackson 1993). It has been suggested (Rogallo, private communication) that the discrepancy between the numerical and experimental values may result from the relatively small number of numerical modes in the simulation (64^3) which robs the cascade of the interactions with the low wavenumber modes at scales larger than the size of the computational box. If that were so, the correct value would be approached for larger simulations. A single experiment in a 128^3 box, using the same subgrid mode, gave a slightly lower constant in the range 1.75-1.85, but the difference was too small for a definite conclusion.
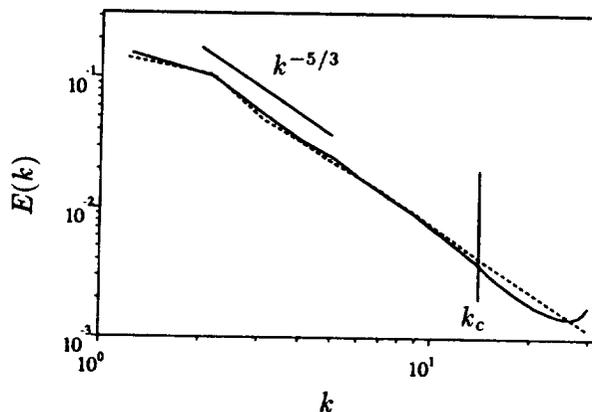
FIGURE 4. Equilibrium three-dimensional energy spectrum for 64^3 numerical boxes in which energy is forced both at the low wavenumber shell, and for modes above $k_c = k_{max}/2$. ——— : Total energy in the high shell extrapolated to $k^{-5/3}$. - - - - : Energy spectrum in high shell extrapolated. Vertical line is limit of damped shell. Turbulent viscosity in both cases: $\alpha/\alpha_0 = 0.8$.

In any case, these experiments suggest that, besides the constant eddy viscosity introduced to model the interaction with the very small scales, all that is needed to correctly model the dissipation at high Reynolds numbers is to have a "sacrificial" spectral shell with the right amount of energy, just beyond the scales of interest. The nonlinear interactions with the modes in that shell mimic those with scales just below the fully resolved ones in the real flow. It is important to realize that there is little reason to expect the modes in the damped shell to be correctly computed and that they should be filtered out when flow statistics higher than the energy are calculated.

For the infinite Reynolds number case studied here, the optimum damping strategy seems to be to constrain the spectrum in the sacrificial shell to the extrapolated $k^{-5/3}$ law. Other similar strategies can probably be developed for flows at lower Reynolds numbers. While this is trivial to implement in the present isotropic spectral code, it is interesting to inquire whether the energy transfer outside the damped shell is sensitive to the detailed form of the constrained spectrum, or whether a simpler strategy might be used.

Figure 4 shows the results of an experiment in which the total energy in the last shell ($k > k_c = k_{max}/2$), rather than its spectrum, was used as a constraint, with the extra addition of the eddy viscosity of Fig. 3. The total energy is adjusted to the one that would be contained in the damped layer if its spectrum were extrapolated from $E(k_c)$ according to the $k^{-5/3}$ law. The optimum simulation from Fig. 3 is also included for comparison, and the results are seen to differ little outside the damped layer.

From a practical point of view, this scheme is much simpler that the full $k^{-5/3}$ one since it involves only the calculation of a single global energy and of a single

damping factor. It could, in principle, be implemented in a finite difference code by the use of appropriate filters.

3. Backscatter

The results in the previous section are consistent with the classical idea that the interaction of a given range of turbulent scales with features of much smaller size can be approximately modeled by an eddy viscosity, even though the interaction between similar scales can not. A common scheme for the modeling of these near interactions is to separate them into an enhanced wave-number dependent eddy viscosity and a backscatter component which moves energy from the small to the large scales (Kraichnan 1976, Leslie & Quarini 1979). The backscatter component is sometimes represented as a random stirring force (Chasnov 1991) because it can be shown that the effect of such a force is always to feed energy into the flow. The separation into forward and backward cascade has been re-encountered recently in a different context. When a direct simulation of turbulence is divided into large and small scale components by filtering the velocity field, the flow of energy between the two components is found to be randomly positive and negative at different *spatial* locations in the flow, so that the global energy drain to the small scales is only the small residue from two large terms of opposite sign (Piomelli *et al.* 1991). It has also been shown that most of this random energy exchange is dominated by interactions among structures separated at most by a factor of two in wavenumber magnitude (Domaradzki, Liu & Brachet 1993).

There is no clear correspondence between the two different definitions of backscatter, and in fact, it can be argued that the existence of regions of positive and negative energy transfer has little to do with the presence of a cascade. It is easy to find examples of steady laminar flows in which there is no net transfer of energy, but which contain regions of localized forward and backward "cascade". An examination of such flows might be useful in understanding more complicated situations. We will discuss a simple example which admits an analytical solution.

Consider a velocity field u which is decomposed into large and small scale components by means of a circular box filter

$$G(x) = 1/\pi a^2 \quad \text{if } |x| < a, \qquad G(x) = 0 \quad \text{otherwise.} \tag{6}$$

Denote filtered, large scale, variables by an overbar. The subgrid Reynolds stress is defined as

$$\tau_{ij} = \overline{u_i u_j} - \overline{u}_i \overline{u}_j. \tag{7}$$

It is also possible to define a large scale rate of strain tensor

$$\overline{S}_{ij} = (\overline{u}_{i,j} + \overline{u}_{j,i})/2, \tag{8}$$

and a local subgrid "Reynolds" energy transfer rate

$$Q = \tau_{ij} \overline{S}_{ij}. \tag{9}$$

This term appears on the right hand side of the energy equation for the large scales and, with the opposite sign, on that for the small scales. Consider now a simple steady two dimensional flow formed by a point vortex, of circulation γ, located at the origin in the pure straining field

$$u_1 = -\sigma x_2, \qquad u_2 = -\sigma x_1. \tag{10}$$

It is easy to see that the effect of the filter on the point vortex is to spread it into a circular patch of uniform vorticity $\omega_a = \gamma/4\pi a^2$ with radius $2a$, while the straining flow (10) is left invariant. The full Reynolds stress and rate of strain tensors can be computed explicitly (see Appendix) and the dominant terms near the origin are

$$\tau_{ij} = \frac{\gamma^2 \log(a/r)}{2\pi^2 a^2} \begin{pmatrix} \sin^2 \phi & -\sin \phi \cos \phi \\ -\sin \phi \cos \phi & \cos^2 \phi \end{pmatrix}, \tag{11}$$

which is due to the vortex, and

$$\overline{S}_{ij} = \begin{pmatrix} 0 & -\sigma \\ -\sigma & 0 \end{pmatrix}, \tag{12}$$

which is due to the stagnation flow, where (r, ϕ) are polar coordinates based on (x_1, x_2). When $r \ll a$, the transfer term behaves as

$$Q = \frac{\gamma^2 \sigma}{2\pi^2 a^2} \log(a/r) \sin 2\phi, \tag{13}$$

which is not zero pointwise even though its integral vanishes identically when taken over the whole plane, as it must for any stationary flow.

The interpretation is easy. The small scales of the flow lie near the vortex, where gradients are large. The vortex alone produces no transfer since fluid particles follow circular trajectories at a constant distance from the center and, therefore, remain at the same "scale". When the stagnation flow is added, the particles move towards the vortex when they pass near $\phi = \pi/4$ or $5\pi/4$, and away from it when they pass near $\phi = 3\pi/4$ or $7\pi/4$. In the first case, the particle moves from a large scale to a small scale environment, and the energy appears to cascade to higher wave numbers. In the second case, the opposite is true, and the cascade is reversed. Note that in reality there is only a reversible deformation of fluid particles as they are carried by the flow into regions in which the dominant local gradients are larger or smaller. It can be shown that in situations less symmetric than the one discussed here, the energy exchange is most active when the scales of the advecting flow are roughly similar to those of the flow generating the gradients. The "true" cascade, resulting in an irreversible transfer of energy from one scale to another, comes from those interactions in which the two scales are very different and in which the deformations are not reversible. The idea that most of the interaction between neighboring scales is not a simple energy diffusion process was put forward forcibly by Kraichnan (1976), Rose (1977), and many others afterwards.

The situation is complicated further because the quantity Q is only part of the real subgrid energy flux $\epsilon(x,\ t) = -D(\bar{u}^2/2)/Dt$, although it is often used to represent the entire flux because the volume integrals of the two are the same. The local difference, which contains the divergence of pressure-velocity and stress-velocity products, can be of the same order of magnitude as the flux itself, and in fact, it is easily seen that the sign of (13) is not even necessarily the same as that of the real transfer because it is compensated by the divergence terms. A consequence is that while it makes sense to speak of energy transfer over large volumes of the fluid or of transfer between widely separated scales in which the surface terms tend to cancel statistically, the *local* energy transfer due to the type of eddy advection displayed by the previous example is a poorly defined quantity that may be difficult to model in any locally deterministic way. The procedure outlined in the previous section avoids this by providing a model for the subgrid scales rather than trying to model the stresses that they produce.

4. Discussion and future work

We have shown that, at least for the calculation of the energy spectrum, isotropic turbulence at high Reynolds numbers can be modeled rather simply by damping a high wavenumber spectral shell in such a way that the energy it contains is the same as that which would be contained in a corresponding shell within an inertial range. The simulations are improved somewhat by the addition of a constant eddy viscosity to account for the nonlinear interactions with scales smaller than those contained in the constrained shell. The magnitude of the viscosity coefficient is a function of the energy in the last spectral shell and agrees approximately with the predictions of EDQNM calculations. The interactions with the flow scales in the constrained shell are approximately accounted for by providing that shell with the right energy, and they include all the backscatter from small to large scales since the effect of the eddy viscosity is purely dissipative.

The effect on the resolved scales of varying the normalized eddy viscosity, the only adjustable parameter in the model, is slight (Fig. 3) although it has a large effect on the behavior of the damped shell. This is best explained by the fact that most of the energy transferred from the resolved scales goes into the spectral octave immediately below it, but that the scales themselves are insensitive to the eventual fate of the energy once it has been transferred. For example, in both of the simulations in Fig. 4, approximately 72% of the energy is lost to the damped shell while only the remaining 28% is withdrawn directly from the resolved scales by the eddy viscosity. These values are broadly comparable to those predicted by the simplified analysis of Tennekes & Lumley (1972), who on the basis of qualitative arguments about the physical mechanism of the cascade, conclude that the energy transfer between shells with wave numbers k and $k' > k$ should vary as $(k/k')^{7/3}$. This behavior has been verified in (Zhou 1993) for shells with large wave number disparities. An integration of that law results in a prediction that 61% of the transfer should go to the next wave number octave.

The insensitivity of the resolved scales to the details of the energy dissipation in the damped shell can be seen from the comparatively small differences between their

C-3

spectra in the $\alpha = 0$ and $\alpha/\alpha_0 = 0.8$ simulations in Fig. 3. The energy budgets of the damped shell in both cases are very different. For $\alpha = 0$, energy is removed only from the damped shell by the damping factor, while for $\alpha/\alpha_0 = 0.8$, 28% is removed from the resolved scales by viscosity, 52% is removed by viscosity from the damped shell, and only the remaining 20% is removed by the damping factor. It is this locality of the energy transfer, coupled with insensitivity to the details of the unresolved energy shells, that makes modeling practical.

The present set of experiments belongs to the recently developed class in which part of the flow field is computed as auxiliary to the calculation of the largest scales and eventually discarded. The best known of them is the Dynamic model in (Germano *et al.* 1991). In that model, the subgrid dissipation is modeled by an eddy viscosity whose magnitude is computed by enforcing similarity of two different scales of the flow. Because the similarity is applied locally, the presence of pointwise backscatter results in locally negative viscosity coefficients that cause numerical problems. It follows from the arguments in §3 that such diffusive models for the backscatter are unlikely to be successful.

We have followed a different route in that we have simulated the near interactions by providing an actual energy shell of roughly the right amplitude with which the flow can interchange energy naturally. There is no guarantee that the flow structures whose scales are in this shell are correctly computed, and they should be filtered before the results are used. This is true of the smallest scales in most LES calculations. On the other hand, the present scheme is intrinsically dissipative and unlikely to develop numerical instabilities. As in the Dynamic model, most of the dissipation is computed from the flow parameters themselves, and the residual eddy viscosity can be computed from analytic arguments. Furthermore, since the eddy viscosity scales with the turbulent energy, the laminar limit is contained in the model. Although the discussion in this paper is framed in terms of a spectral approach, it is indicated at the end of §2 how the model could be adapted to finite difference codes.

The experience gained in this work provides some insight into the reasons for the success of the Dynamic model in many situations. The similarity assumption in the Dynamic model essentially provides the right eddy viscosity for a smooth extrapolation of the spectrum of the resolved scales (the "test" filter) into the smaller scales and, therefore, provides a high wavenumber component with the right extrapolated energy. We have shown here that this seems to be enough to provide the field with the right dissipation.

The present model has been developed as a research tool for the study of energy transfer in isotropic turbulence and has only been tested on low order statistics. Since most high order statistical moments are known to be dominated by the small scales of the flow, they are unlikely to be captured correctly by this, or by any, LES model. More important, we have only dealt with homogeneous turbulence, and as outlined in the introduction, there are reasons to believe that some of the conclusions might not be directly applicable to inhomogeneous situations. In particular, the crucial independence of the large scale flow from the small scale details may not be

true in any local sense for those cases. Clearly, much more work is needed in all those directions.

Acknowledgements

REFERENCES

BATCHELOR, G. K. 1953 *The theory of homogeneous turbulence.* Cambridge Univ. Press.

BELL, T. L. & NELKIN, M. 1978 Time dependent scaling relations and a cascade model of turbulence. *J. Fluid Mech.* **88**, 369-391.

BERMAN, N. S. 1978 Drag reduction by polymers. *Ann. Rev. Fluid Mech.* **10**, 47-64.

CANUTO, C., HUSSAINI, M. Y., QUARTERONI, A. & ZANG, T. A. 1987 *Spectral methods in fluid dynamics.* Springer, pp. 85-86.

CHASNOV, J. R. 1991 Simulation of the Kolmogorov inertial subrange using an improved subgrid model. *Phys. Fluids.* **A 3**, 188-200.

DEAN, R. B. 1978 Reynolds number dependence of skin friction and other bulk flow variables in two-dimensional rectangular ducts. *J. Fluid Eng.* **100**, 215-223.

DOMARADZKI, J. A., LIU, W. & BRACHET, M. E. 1993 An analysis of subgrid-scale interactions in numerically simulated isotropic turbulence. *Phys. Fluids.* **A 5**, 1747-1759.

FORNBERG, B. 1977 A numerical study of two-dimensional turbulence. *J. Comput. Phys.* **25**, 1-31.

GERMANO, M., PIOMELLI, U., MOIN, P. & CABOT, W. H. 1991 A dynamic subgrid scale eddy viscosity model. *Phys. Fluids.* **A 3**, 1760-1765. Erratum, *Phys. Fluids* A **3**, 3128.

JIMÉNEZ, J., WRAY, A., SAFFMAN, P. G. & ROGALLO, R. S. 1993 The structure of intense vorticity in isotropic turbulence. *J. Fluid Mech.* **255**, 65-90.

KRAICHNAN, R. H. 1976 Eddy viscosity in two and three dimensions. *J. Atmos. Sci.* **33**, 1521-1536.

KOLMOGOROV, A. N. 1941 The local structure of turbulence in incompressible viscous fluids a very large Reynolds numbers. *Dokl. Nauk. SSSR.* **30**, 301-305 (see e.g. L. D. Landau & E. M. Lifshitz, 1959, *Fluid mechanics*, Pergamon, 116-123).

LEE, T. D. 1952 On the statistical properties of hydrodynamics and magneto-hydrodynamical fields. *Quart. App. Math.* **10**, 69-74.

LEITH, C. E. 1967 Diffusion approximation to inertial energy transfer in isotropic turbulence. *Phys. Fluids.* **10**, 1409-1416.

LESIEUR, M. 1990 *Turbulence in fluids.* Kluwer.

LESIEUR, M. & ROGALLO, R. S. 1989 Large eddy simulation of passive scalar diffusion in isotropic turbulence. *Phys. Fluids.* **A 4**, 718-722.

LESLIE, D. C. & QUARINI, G. L. 1979 The application of turbulence theory to the formulation of subgrid scale procedures. *J. Fluid Mech.* **91**, 65-91.

PIOMELLI, U., CABOT, W. H., MOIN, P. & LEE, S. 1991 Subgrid-scale backscatter in turbulent and transitional flows. *Phys. Fluids.* **A 3**, 1766-1771.

ROGALLO, R. S. 1981 Numerical experiments in homogeneous turbulence. *NASA Tech. Mem.* **81315.**

ROSE, H. A. 1977 Eddy diffusivity, eddy noise and subgrid scale modeling. *J. Fluid Mech.* **81**, 719-734.

SHE, Z-S., JACKSON, E. 1993 A constrained Euler system for Navier Stokes turbulence. *Phys. Rev. Lett.* **70**, 1255-1258.

SREENIVASAN, K. R. 1984 On the scaling of the turbulence energy dissipation rate. *Phys. Fluids.* **27**, 1048-1051.

SHTILMAN, L. & CHASNOV, J. R. 1992 LES vs. DNS: a comparative study, *Summer Program Proceedings-1992*, Center for Turbulence Research, Stanford Univ./NASA Ames, 137-143.

TENNEKES, H. & LUMLEY, J. L. 1972 *A first course in turbulence*, MIT Press, pp. 260-261.

WALSH, M. J. 1990 Riblets, in *Viscous drag reduction in boundary layers*, edited by D. M. Bushnell and J. N. Hefner. AIAA, pp. 203-261.

YOSHIZAWA, A. 1982 A statistically derived subgrid model for the large-eddy simulation of turbulence. *Phys. Fluids.* **25**, 1532-1538.

ZHOU, Y. 1993 Interacting scales and energy transfer in isotropic turbulence. *Phys. Fluids.* **A 5**, 2511-2524.

Appendix: Energy transfer in a simple stationary flow

We present here the detailed analysis of the flow discussed in §3, formed by a point vortex at the stagnation point of a straining flow in eq. (10). We define polar coordinates (r, ϕ), but express all vectors and tensors as components on the Cartesian axes (x_1, x_2). The velocity field due to the vortex is given by

$$u_v = \frac{\gamma}{2\pi r} (\sin\phi, -\cos\phi), \qquad (A-1)$$

and that due to the straining flow is

$$u_s = -\sigma r (\sin\phi, \cos\phi). \qquad (A-2)$$

After filtering, the vortex becomes a uniform circular vortex patch. We will only be interested in the behavior of the energy inside the patch, where $r \leq 2a$. The filtered velocity is

$$\overline{u}_v = \frac{\gamma r}{8\pi a^2} (\sin\phi, -\cos\phi), \qquad (A-3)$$

while the filtered straining flow is equal to itself because of linearity. The Reynolds stresses are computed according to equation (7) and contain terms coming from the interaction of the vortex with itself, from the interaction of the straining flow with itself, and from the mutual interaction,

$$\tau_{vv} = \frac{\gamma^2}{4\pi^2 a^2} \left[\log\left(\frac{a^2}{r^2} - 1\right) - \frac{r^2}{16a^2} \right] \begin{pmatrix} \sin^2\phi & -\sin\phi\cos\phi \\ -\sin\phi\cos\phi & \cos^2\phi \end{pmatrix}, \qquad (A-4)$$

$$\tau_{vs} = \frac{\gamma\sigma}{\pi} \left[1 - \frac{r^2}{4a^2} \right] \begin{pmatrix} -\sin^2\phi & 0 \\ 0 & \cos^2\phi \end{pmatrix}, \qquad (A-5)$$

$$\tau_{ss} = \frac{\sigma^2 a^2}{2} \begin{pmatrix} \sin^2\phi & -\sin\phi\cos\phi \\ -\sin\phi\cos\phi & \cos^2\phi \end{pmatrix}. \qquad (A-6)$$

The dominant term when $r \ll a$ is the logarithmic term in (A-4), which is reflected in eq. (11) in the body of the paper. In the same way, the filtered rate of strain tensor has a term coming from the vortex and another coming from the straining field,

$$\overline{S}_v = \frac{-\gamma}{16\pi a^2} \begin{pmatrix} -\sin 2\phi & \cos 2\phi \\ \cos 2\phi & \sin 2\phi \end{pmatrix}, \qquad (A-7)$$

$$\overline{S}_s = -\sigma \begin{pmatrix} 0 & 1 \\ 1 & 0 \end{pmatrix}. \qquad (A-8)$$

Both are of the same order near the origin, but (A-7) is orthogonal to the dominant stress, and the vortex does not generate energy transfer when interacting with itself. The "Reynolds" transfer, Q, near the origin is given by eq. (13).

Most of this transfer, however, is spurious and cancels with various divergence terms in the energy equation. The real transfer of kinetic energy from the subgrid scales into the filtered flow field is

$$-\epsilon = \frac{D\overline{u}^2/2}{Dt} = \overline{u} \cdot \nabla\overline{u}, \qquad (A-9)$$

and can be computed exactly as

$$-\epsilon = \sigma \left(\frac{\gamma^2}{64\pi^2 a^4} - \sigma^2 \right) r^2 \sin 2\phi. \qquad (A-10)$$

Its angular structure is the same as that of Q, but its sign depends on the balance between the increase of the azimuthal velocity as a particle approaches the vortex and the decrease of its radial velocity as it approaches the stagnation point.